ELSEVIER

Journal of Power Sources 63 (1996) 97–102

JOURNAL OF POWER SOURCES

Studies on the Li–Mn–O spinel system (obtained from melt-impregnation method) as positive electrodes for 4 V lithium batteries. Part III. Characterization of capacity and rechargeability

Yongyao Xia, Masaki Yoshio *

Department of Applied Chemistry, Saga University, Saga 840, Japan

Received 24 May 1996; accepted 22 July 1996

Abstract

A series of 'lithium-rich' or 'oxygen-rich' spinel compounds are prepared from the reaction of $LiNO_3$ with electrochemically prepared manganese dioxide (EMD) via the melt-impregnation method. The capacity and rechargeability of these compounds are semi-quantitatively discussed in terms of an $LiMn_2O_4$–$Li_4Mn_5O_{12}$–$Li_2Mn_4O_9$ phase diagram. The capacity decreases as the lithium or oxygen content increases in the spinel matrix. By contrast, the rechargeability is improved.

Keywords: Lithium; Lithium-ion batteries; Spinel; Manganese dioxide

1. Introduction

In previous work [1,2], we have reported the synthesis and electrochemical behaviour of optimum spinel electrodes obtained from $LiNO_3$, LiOH and various manganese dioxides by the melt-impregnation method. Although the capacity and rechargeability have been improved greatly, capacity fading on cycling has been observed for stoichiometric spinel compounds of $LiMn_2O_4$. By contrast, 'lithium-rich' or 'oxygen-rich' compounds exhibit good rechargeability. The problem is that these non-stoichiometric spinels always deliver slightly lower capacity [2–5]. Consequently, this raises the issue of how to optimize both the capacity and rechargeability of the spinel compound for use as a practical 4 V positive electrode for lithium-ion batteries. The aim of the present study is to demonstrate the relationship between the capacity, the rechargeability and the method of preparation, as indicated by the Li–Mn–O phase diagram.

2. Experimental

Each sample was prepared by the melt-impregnation method, as reported previously [1,6]. The synthesis of each compound is given in Section 3.1 below. All compounds were prepared by the reaction of electrochemically prepared manganese dioxide (EMD) with $LiNO_3$.

The composition of each sample was characterized by atomic adsorption spectroscopy and chemical analysis. The manganese valency was calculated by analysis of the total manganese and oxidation powers of the manganese ions according to Kozawa's method [7]. The oxygen content was evaluated from the lithium ion and manganese ion contents. The X-ray powder diffraction technique was used to determine the crystal structure. The X-ray diffraction data were collected on a Rigaku RINT 1000 X-ray diffractometer (Rigaku, Japan) with Fe Kα radiation.

The electrochemical cell was the same as that described previously [1]. The cathode consisted of 25 mg active material and 15 mg conducting binder (acetylene black-polytetrafluoroethylene composite). The electrolyte solution was 1 M $LiPF_6$–EC/DMC (1:2 in volume) (note, EC: ethylene carbonate and DMC: dimethyl carbonate). The cycling tests for each $Li/LiMn_2O_4$ cell were performed on a CR2032-type button cell. The typical current rate was $C/3$ (40 mA g^{-1}), except where otherwise specified. All cell assemblies were carried out in a dry box filled with argon gas. Other sets of experimental conditions are given below.

* Corresponding author.

PII S0378-7753(96)02455-X

3. Results and discussion

3.1. Syntheses of $Li_{1+x}Mn_2O_{4+y}$ ($x \geq 0$, $y \geq 0$) compounds

An isothermal cross section of the Li–Mn–O phase diagram was first reported by Thackeray et al. [8]. The spinel structure Li–Mn–O system is defined by Mn_3O_4–$Li_4Mn_5O_{12}$–λ-MnO_2 [8]. The compounds applied in 4 V Li cell positive electrodes lie in the $LiMn_2O_4$–$Li_4Mn_5O_{12}$–λ-MnO_2 plane [9]. In fact, λ-MnO_2 cannot be obtained directly from lithium salt and manganese oxides by a solid–solid reaction, which is the limitation of $LiMn_2O_4$ with all Li^+ ions extracted from the 8*a* tetrahedral sites by an electrochemical [10] or a chemical method [11]. The occupation of manganese in 16*d* octahedral sites and O in the 32*e* octahedral sites is the same as for $LiMn_2O_4$. Therefore, it may be preferable to refer to a practical 4 V electrode as one that is located on the $LiMn_2O_4$–$Li_4Mn_5O_{12}$–$Li_2Mn_4O_9$ plane. We found that each compound can be synthesized directly by a solid–solid reaction in which the Li/Mn molar ratio, reaction temperature and time are all controlled.

The reaction mechanism for the spinel compound obtained from $LiNO_3$ and MnO_2 has been discussed in a previous report [12]. Disordered spinel was formed at 420 °C. This disordered spinel transforms to a well-ordered spinel via loss of oxygen when the temperature is raised. The optimum synthesis condition for the spinel compound is preheating the mixture of $LiNO_3$ and EMD to 260 °C. This process allows the melted $LiNO_3$ to impregnate into the MnO_2 pores. On further heating at 425 °C the disordered spinel is formed. The final heating temperature depends on the required composition. Here, the stoichiometric spinel is defined as $LiMn_2O_4$, and the non-stoichiometric spinel as the compounds that are 'lithium-rich' $Li_{1+x}Mn_{2-y}O_4$ ($x>0, y>0$) or 'oxygen-rich' $Li_{1-x}Mn_{2-y}O_4$ ($x>0, y>0$). Apparently, $Li_4Mn_5O_{12}$ is the limiting compound of the lithium-rich variety, and $Li_2Mn_4O_9$ is the limiting compound of the oxygen-rich variety for a 4 V cathode. The detailed conditions for the preparation of the compounds, i.e. stoichiometric $LiMn_2O_4$, lithium-rich $Li_{1+x}Mn_{2-x}O_4$ ($0<X<0.33$) and oxygen-rich $Li_{1-x}Mn_{2-2x}O_4$ ($0<X<0.11$), are given in Tables 1 and 2. The chemical composition for each compound was determined by chemical analysis. The results are shown in Table 3 and Fig. 1. In the latter, the length of the straight line (b) represents the Li/Mn molar ratio and average Mn valency, line (a) the average Mn valency, and line (c) the Li/Mn molar ratio. It is evident that the stoichiometric spinel $LiMn_2O_4$ and non-stoichiometric spinels $Li_2Mn_4O_9$ and $Li_4Mn_5O_{12}$ are located on the equal length triangle.

The oxygen-rich compounds are located on the tie-line in the Li–Mn–O phase diagram between $LiMn_2O_4$ and $Li_2Mn_4O_9$ (line (a) in Fig. 1). The oxygen content in the spinel matrix increases with decrease in the heating temperature, and thus causes the average Mn valency to increase from 3.5 to 4.0. It was intended to prepare a lithium-rich compound with the common formula $Li_{1+x}Mn_{2-x}O_4$, as described by Thackeray et al. [4] and Gao and Dahn [13], but it is very difficult to obtain such a composition in which the total number of Mn and Li atoms is just equal to 3 per unit. In the fact, the number of Li and Mn atoms per unit

Table 1
Synthesis conditions for oxygen-rich compounds

Sample no.	Synthesis conditions
A	260 °C, 5 h; 425 °C, 5 h; 750 °C, 30 h
B	260 °C, 5 h; 425 °C, 5 h; 750 °C, 20 h
C	260 °C, 5 h; 425 °C, 5 h; 700 °C, 20 h
D	260 °C, 5 h; 425 °C, 5 h; 650 °C, 15 h
E	260 °C, 5 h; 425 °C, 5 h; 600 °C, 10 h
F	260 °C, 5 h; 425 °C, 5 h; 550 °C, 10 h
G	260 °C, 5 h; 425 °C, 5 h; 500 °C, 5 h

Table 2
Synthesis conditions for lithium-rich spinel compounds

Sample no.	Synthesis conditions
H	Li/Mn = 0.52; 260 °C, 5 h; 425 °C, 5 h; 750 °C, 10 h
I	Li/Mn = 0.55; 260 °C, 5 h; 425 °C, 5 h; 725 °C, 10 h
J	Li/Mn = 0.60; 260 °C, 5 h; 425 °C, 5 h; 700 °C, 10 h
K	Li/Mn = 0.65; 260 °C, 5 h; 425 °C, 5 h; 600 °C, 10 h
L	Li/Mn = 0.70; 260 °C, 5 h; 425 °C, 5 h; 550 °C, 10 h
M	Li/Mn = 0.75; 260 °C, 5 h, 425 °C, 5 h; 500 °C, 10 h
N	Li/Mn = 0.80; 260 °C, 5 h; 425 °C, 5 h; 450 °C, 10 h

Table 3
Chemical composition of oxygen-rich and lithium-rich compounds

Sample no.	$Li_{1-x}Mn_{2-x}O_4$ or $LiMn_2O_{4+y}$		Sample no.	$Li_{1+x}Mn_{2-x}O_4$ ($Li_{1+x}Mn_{2-y}O_4$)	
	x	y		x	y
A	0.002	0.009	H	0.020	0.031
B	0.003	0.012	I	0.051	0.088
C	0.007	0.030	J	0.120	0.133
D	0.012	0.048	K	0.171	0.198
E	0.016	0.065	L	0.230	0.243
F	0.018	0.072	M*	0.294	0.275
G	0.026	0.107	N*	0.361	0.299

* Samples M and N were slightly deficient in oxygen.

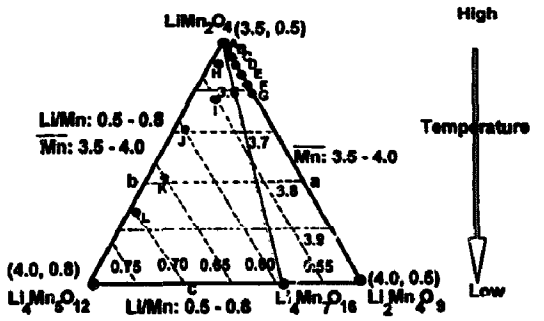

Fig. 1. Chemical composition of compounds located on the $LiMn_2O_4$–$Li_4Mn_5O_{12}$–$Li_2Mn_4O_9$ plane: (A) $LiMn_2O_{4.009}$; (B) $LiMn_2O_{4.012}$; (C) $LiMn_2O_{4.030}$; (D) $LiMn_2O_{4.048}$; (E) $LiMn_2O_{4.065}$; (F) $LiMn_2O_{4.072}$; (E) $LiMn_2O_{4.107}$; (H) $Li_{1.020}Mn_{1.969}O_4$; (I) $Li_{1.051}Mn_{1.912}O_4$; (J) $Li_{1.120}Mn_{1.876}O_4$; (K) $Li_{1.171}Mn_{1.802}O_4$; (L) $Li_{1.230}Mn_{1.757}O_4$; (M*) $Li_{1.294}Mn_{1.725}O_4$; (N*) $Li_4Mn_5O_{12-0.245}$.

depends not only on the Li/Mn molar ratio in the starting materials but also on the oxygen content, as the compounds are located on line (a) and have the same Li/Mn molar ratio (Li/Mn = 0.50), but different composition by virtue of the different heating temperature. The lithium-rich compounds are located on line (b) in Fig. 1. It should be noted that the compounds with much higher lithium contents, such as samples M and N, are slightly deficient in oxygen under the current synthesis conditions. As these compounds are usually employed for 3 V positive electrodes, they are considered in detail in this work. The compounds located on line (c) are lithium-rich and oxygen-rich compounds, in which the averaged valency of Mn in the compound is 4. The composition of each compound located on the $LiMn_2O_4$–$Li_4Mn_5O_{12}$–$Li_2Mn_4O_9$ triangle plane is written as

$$Li_{8n/(n+m)}Mn_{8/(n+m)}O_4 \quad (0.5 \le n \le 0.8,\ 3.5 \le m \le 4.0) \tag{1}$$

where n is the Li/Mn molar ratio, m is the average Mn valency. All compounds located on the $LiMn_2O_4$–$Li_4Mn_5O_{12}$–$Li_2Mn_4O_9$ plane can be divided into two groups: (i) the compounds on the $LiMn_2O_4$–$Li_4Mn_5O_{12}$–$Li_4Mn_7O_{16}$ plane are lithium-rich compounds, in which lithium ions are present at 8*a* tetrahedral and 16*d* octahedral sites, and (ii) the compounds on the $LiMn_2O_4$–$Li_2Mn_4O_9$–$Li_4Mn_7O_{16}$ plane are oxygen-rich compounds, in which vacancies are present at both tetrahedral and octahedral sites.

3.2. Initial capacity

It is common knowledge that the charge and discharge capacity for spinel structure electrodes are dependent on the inserted/extracted amount of Li^+. Removal and insertion of the lithium ions from the spinel framework is accompanied by a redox process between Mn^{3+} and Mn^{4+}. The total amount of extracted lithium ions should be directly related to the Mn^{3+} content in the compound. The initial charge capacity can be evaluated through a knowledge of the Li/Mn molar ratio and the average Mn valency, m. It is assumed that the

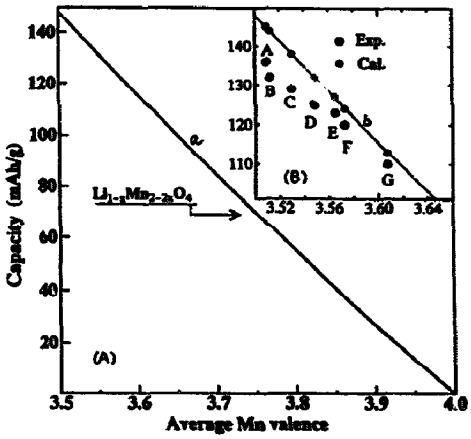

Fig. 2. Initial capacity vs. average Mn valency of oxygen-rich compounds.

theoretical capacity for $LiMn_2O_4$ is 148 mAh g^{-1} for 1 mole of lithium ions extracted from the spinel framework, which corresponds to 1 mole of Mn^{3+} oxidized to Mn^{4+}, i.e.

$$Li[Mn^{3+}Mn^{4+}]O_4 - Li^+ \rightarrow 2\lambda\text{-}MnO_2 \tag{2}$$

The relationship between the average Mn valence and the calculated initial capacity for the oxygen-rich compound, $Li_{1-x}Mn_{2-2x}O_4$, is displayed in Fig. 2(A) (curve (a)). The initial capacity decreases with increase in the average Mn valency. The calculated initial capacities of the prepared compounds should be located on the upper post of curve (a). To see this more clearly, the calculated capacities of the compounds are given in Fig. 2(B) (curve (b)) together with the measured values. The latter were obtained for a low current-density of 0.1 mA cm^{-2}. It is evident that the compound synthesized at low temperature delivers an initial capacity close to the theoretical value, this is due in part to the larger surface area. On the other hand, a low heating temperature usually causes a higher oxygen content and thus reduces the capacity. Therefore, it is suggested that a suitable heating temperature for an optimum spinel structure is between 600 and 800 °C. As reported by Tarascon et al. [14] and Manev et al. [15], a high heating temperature also reduces the capacity. It should be noted that the effect on oxygen content is not only determined by the heating temperature, but is also influenced by the starting material (lithium salt and MnO_2 source), the heating time and, in particular, the heating atmosphere. As described previously [1], a nitrogen rather than an air atmosphere is conducive to the loss of oxygen at a given temperature.

The relationship between the calculated initial capacity and the Li/Mn molar ratio for $Li_{1+x}Mn_{2-x}O_4$ ($0 \le x \le 0.33$) is given in Fig. 3. The initial capacity decreases with increase in the Li/Mn molar ratio. The calculated and measured capacities for the prepared compounds are also displayed in Fig. 3. Even though the chemical formulae of the compounds did not fit well with $Li_{1+x}Mn_{2-x}O_4$, the initial capacity reduces with increasing lithium content in the spinel matrix.

In summary, it is possible to obtain each compound on $LiMn_2O_4$–$Li_4Mn_5O_{12}$–$Li_2Mn_4O_9$ plane by controlling the

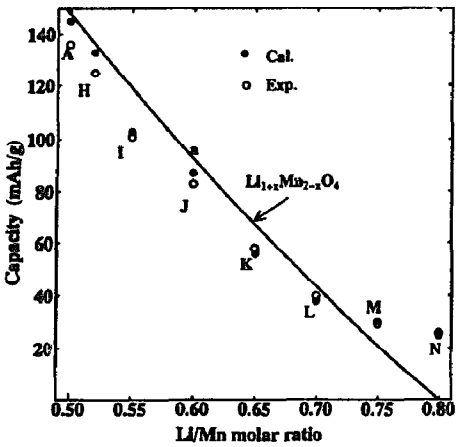

Fig. 3. Initial capacity vs. Li/Mn molar ratio of lithium-rich compounds.

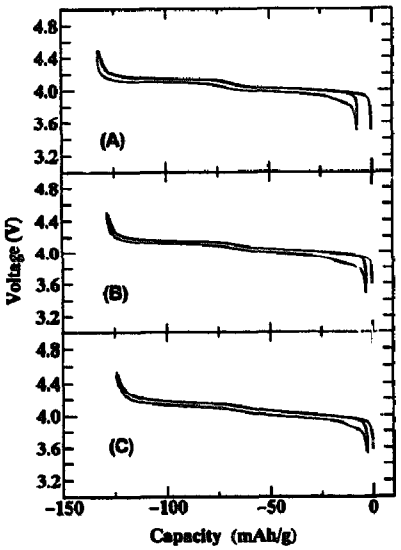

Fig. 4. Typical charge and discharge curves of $Li/LiMn_2O_{4+y}$ cells with various oxygen-rich spinel cathodes: (A) sample A, $LiMn_2O_{4.009}$; (B) sample D, $LiMn_2O_{4.048}$, and (C) sample F, $LiMn_2O_{4.072}$.

synthesis conditions, i.e. Li/Mn molar ratio, temperature, time, etc. The initial capacity decreases with increase in the Li/Mn molar ratio or oxygen content. A given compound has an initial capacity of $1184(4-m)/(m+n)$ mAh g^{-1}, where the definition of n and m is that given in Section 3.1.

3.3. Charge and discharge profile

It is easily anticipated that any difference in chemical composition may cause a different crystal structure. This, in turn, will affect the charge and discharge behaviour of an $Li/Li_xMn_2O_4$ cell. To confirm this, tests have been made on oxygen-rich compounds (samples A, D, F) and lithium-rich compounds (samples H, I, J). Typical charge and discharge curves of an $Li/Li_xMn_2O_4$ cell containing various lithium-rich or oxygen-rich compounds are given in Figs. 4 and 5, respectively. A stoichiometric spinel $LiMn_2O_4$ (sample A, Fig. 4) displays a two-step voltage profile, with plateaus at around 4 V and at about 100 mV apart. As the oxygen content is increased, the shape of the charge and discharge curve gradually transforms to a quasi one-plateau (sample F, $LiMn_2O_{4.072}$); in particular, it occurs in the high-voltage region, where the 'L-shape' curve for sample A changes to a 'S-shape' curve for the oxygen-rich compound, sample F. The same phenomena were also observed for the lithium-rich compounds. As shown in Fig. 5, the high-voltage plateau becomes less visible with increase in lithium content, and the two-step character of the voltage profile totally disappears when the Li/Mn molar ratio reaches 0.60. This can be seen more clearly in differential chronopotentiometric curves (DCC). The data in Figs. 4 and 5 are represented as DCC curves in Figs. 6 and 7, respectively. The peak in the high-

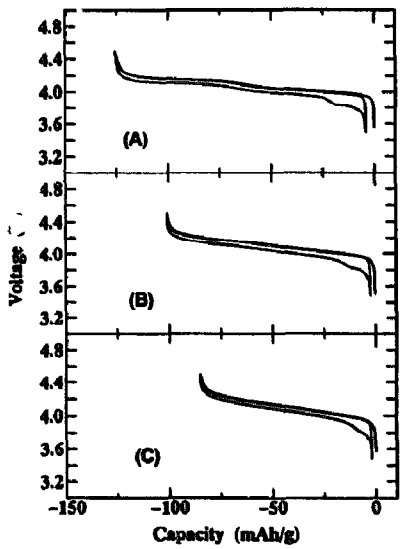

Fig. 5. Typical charge and discharge curves of $Li/Li_{1+x}Mn_{2-y}O_4$ cells with various lithium-rich spinel cathodes: (A) sample H, $Li_{1.020}Mn_{1.969}O_4$; (B) sample I, $Li_{1.051}Mn_{1.912}O_4$, and (C) sample J, $Li_{1.120}Mn_{1.867}O_4$.

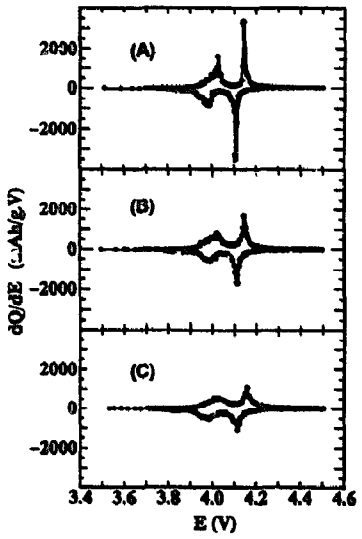

Fig. 6. Differential capacity curves for $LiMn_2O_{4+y}$: (A) sample A; (B) sample D, and (c) sample F. The data were taken from the results given in Fig. 4.

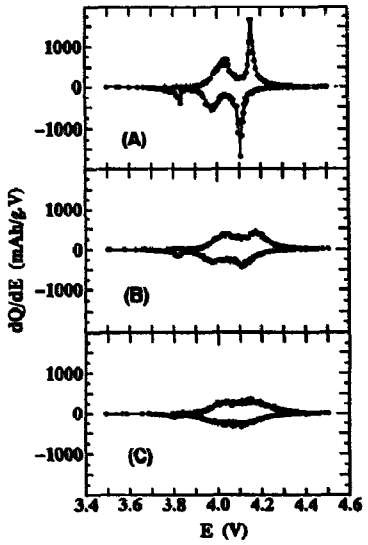

Fig. 7. Differential capacity curves for $Li_{1+x}Mn_{2-y}O_4$: (A) sample H; (B) sample I, and (C) sample J. The data were taken from the results given in Fig. 5.

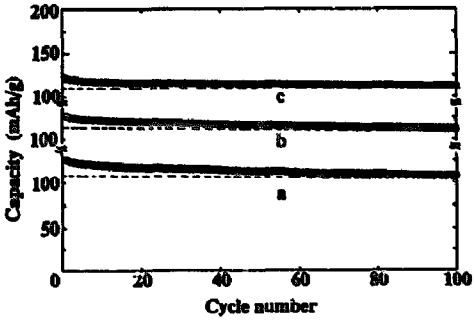

Fig. 8. Cycling behaviour of $Li/LiMn_2O_{4+y}$ cells with various oxygen-rich electrodes: (a) sample A; (b) sample D, and (c) sample F.

potential region becomes weaker with increasing oxygen or lithium content in the spinel matrix, eventually it virtually disappears (sample J, Fig. 7). The reason why oxygen or lithium content affects the electrochemical behaviour of spinel electrodes is not fully understood; it may be due to the establishment of different environments for lithium-ion insertion/extraction. This is because the insertion/extraction potential depends on the energy of the lithium ions in the tetrahedral sites which, in turn, depends on the energy of the bond between each Li^+ ion and its neighbours.

3.4. Cycling behaviour

The rechargeability of each sample was examined in CR2032 button-type cells. Each cell was cycled at a current rate of *C*/3 between 3.5 and 4.5 V. The specific capacity for each sample is plotted as a function of cycle number in Figs. 8 and 9. As expected, the rechargeability is improved with increase in either oxygen or lithium content in the spinel matrix. The capacity loss over the first 100 cycles varies from about 15% of the initial capacity for sample A to 7% for sample F. Similar behaviour was exhibited by the lithium-

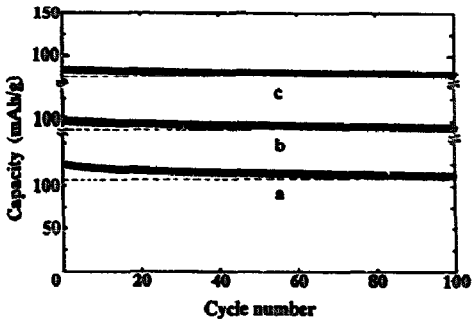

Fig. 9. Cycling behaviour of $Li/Li_{1+x}Mn_{2-y}O_4$ cells with various oxygen-rich electrodes: (a) sample H; (b) sample I, and (c) sample J.

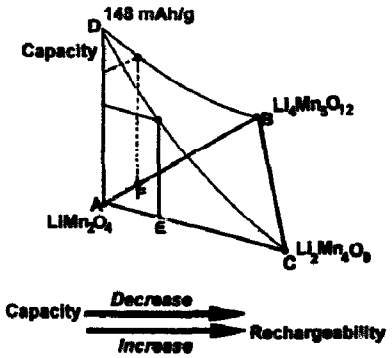

Fig. 10. Three-dimensional diagram of capacity–rechargeability–chemical composition for each compound on $LiMn_2O_4$–$Li_4Mn_5O_{12}$–$Li_2Mn_4O_9$ plane.

rich compounds: the capacity loss was about 10% of the initial capacity for sample H, compared with 5% for sample J. All results reveal that the rechargeability is improved by increase in either the oxygen or lithium content in the spinel matrix.

4. Conclusions

The capacity and rechargeability of a spinel electrode as a 4 V positive electrode for lithium-ion batteries has been semi-quantitatively discussed in terms of an $LiMn_2O_4$–$Li_4Mn_5O_{12}$–$Li_2Mn_4O_9$ phase diagram, as illustrated in Fig. 10. It is concluded that:

(i) each compound located on the $LiMn_2O_4$–$Li_4Mn_5O_{12}$–$Li_2Mn_4O_9$ triangle plane can be prepared by the melt-impregnation method by controlling the conditions of synthesis;

(ii) the initial capacity, *c*, decreases with increasing Li/Mn molar ratio or oxygen content in the spinel matrix, as expressed by Eq. (3), on the other hand, the rechargeability is improved

$$c=\frac{1184(4-m)}{m+n} \quad (3.5\le m\le 4.0,\ 0.5\le n\le 0.8) \qquad (3)$$

(iii) the optimum synthesis conditions for the spinel are a low heating temperature (600 to 800 °C) and a slightly high Li/Mn ratio (> 0.50).

Acknowledgements

The authors thank the Japanese Ministry of Education for grants-in-aid for scientific research nos. 06 453 124 and 06 555 188 that partially supported this research.

References

[1] Y. Xia, H. Takeshige, H. Noguchi and M. Yoshio, *J. Power Sources, 56* (1995) 61.
[2] Y. Xia and M. Yoshio, *J. Power Sources, 57* (1995) 125.
[3] Y. Xia and M. Yoshio, *J. Electrochem. Soc., 143* (1996) 825.
[4] M.M. Thackeray, L.A. de Picciotto, A. de Kock, P. Johnson, V. Nicholas and K. Adendorff, *J. Power Sources, 21* (1987) 1.
[5] G. Pistoia and G. Wang, *Solid State Ionics, 66* (1993) 135.
[6] M. Yoshio, H. Noiguchi, T. Miyashita, H. Nakamura and A. Kozawa, *J. Power Sources, 54* (1995) 483.
[7] A. Kozawa, *Memo. Fac. Nagoya Univ., 11* (1959) 243.
[8] M.M. Thackeray, A. de Kock, M.H. Rossouw and D. Liles, *J. Electrochem. Soc., 139* (1992) 363.
[9] R.J. Gummow and M.M. Thackeray, *J. Electrochem. Soc., 141* (1994) 1178.
[10] T. Ohzuku, M. Kitagawa and T. Hirai, *J. Electrochem. Soc., 137* (1990) 769.
[11] J. Hunter, *J. Solid State Chem., 39* (1981) 142.
[12] M. Yoshio, H. Noguchi, H. Nakamura, Y. Xia, H. Takeshige and K. Ikeda, *Jpn. Electrochem. Soc., 63* (1995) 941.
[13] Y. Gao and J.R. Dahn, *J. Electrochem. Soc., 143* (1996) 100.
[14] J.M. Tarascon, W.R. McKinnon, F. Coowar, T.N. Bowmer, G. Amatucci and D. Guyomard, *J. Electrochem. Soc., 141* (1994) 1421.
[15] V. Manev, A. Momchilov, A. Nassalevska and A. Kozawa, *J. Power Sources, 43–44* (1993) 551.